Global and Planetary Change 170 (2018) 93–105

Contents lists available at ScienceDirect

Global and Planetary Change

journal homepage: www.elsevier.com/locate/gloplacha

Research article

Impact of climate variation on hydrometeorology in Iran

Sanaz Moghim*

Department of Civil Engineering, Sharif University of Technology, Tehran, Iran

ARTICLE INFO

Keywords:
Climate variation
Hydrological cycle
Energy balance
GLDAS
Hydrometeorology
Extreme weather events

ABSTRACT

Results confirm that Iran like many countries is affected by high climate variability, which has influenced hydroclimatological variables such as temperature, evaporation, precipitation, runoff, and radiation. This study uses Global Land Data Assimilation System (GLDAS) data to assess hydrological cycle changes in Iran during a long period (Jan1948-Jan2017). Results show that hydrometeorological variables have significant changes (p-value < .01) during the period of 2010–2017 relative to the baseline period (2004–2009). Most extreme values of these variables including temperature, evaporation, precipitation, wind, and downward longwave radiation occurred recently (in 2015 to 2017). The average temperature of Iran has an upward trend in most months particularly in summer and winter followed by a significant increase of evaporation since 1948 (p-value < .01). Furthermore, the results show significant changes in downward longwave and shortwave radiation, which can be caused by changes in temperature and cloud types. Climate variation has influenced extreme hydrometeorological variables particularly precipitation. The analysis of the results in this study can provide insight into this highly interconnected hydrometeorological changes.

1. Introduction

Climate has been changing globally. Iran like most countries has been experiencing high climate variation, which can change magnitude and trend of hydrometeorological variables. The results of this change like heavy rain, storm, drought, and increase in temperature have been occurring (Tabari et al., 2014). Changes differ from region to region over the country. Abbaspour et al. (2009) used the Soil and Water Assessment Tool (SWAT) model to assess the impact of climate change on Iran's water resources. The results revealed that the southern and eastern regions of the country will be at higher risk of drought while the northern and western regions will be threatened by the floods. Climate variation can affect other sectors such as agriculture and energy directly or indirectly. For instance, the impact of climate variation on the hydrologic cycle can influence hydropower. Jamali et al. (2013) showed that lack of adaptation to climate change leads to considerably decrease of efficiency in the Iran's Karkheh Hydropower in future.

Insufficient climate assessment studies and improper managements lead to environmental degradation and ecosystem/resources (e.g., land, water, air) destruction in Iran. Groundwater depletion in many regions particularly in Northeastern Iran caused subsidence and saltwater intrusion (Motagh et al., 2007). Most lakes in Iran are drying including Lake Urmia, the largest lake in the Middle East and the home of different species (Tourian et al., 2015; Delju et al., 2013; Zarghami, 2011). Dried lake causes sand and dust storm around the lake and affects ecosystem functioning and human health. Dust storm over western Iran has disrupted people's lives (Naimabadi et al., 2016; Najafi et al., 2014). Ecosystem degradation such as coral reef bleaching has been occurring in Persian Gulf (Shinn, 1976; Mostafavi et al., 2007). These issues indicate the necessity of implementing sustainable adaptation and mitigation plans considering possible climate changes.

An increase in temperature variability is predicted by climate models (Bathiany et al., 2018). Higher temperature yields more evaporation and thus increases atmospheric water vapor. Water vapor can produce a wide variety of cloud types with different albedo. Different clouds show varied feedbacks in the energy balance system. For instance, low clouds can block incoming shortwave radiation and decrease surface temperature (negative feedback). On the other hand, high cloud can trap outgoing longwave radiation (positive feedback) and increase surface temperature (Dessler, 2010). Note that the feedbacks of the water vapor and precipitation are very uncertain because precipitation is a highly complex and nonlinear process. Any change in radiation and energy balance (Eq. (1)) affects components of the water cycle (Eq. (2)).

$$R_n = R_S^{\downarrow} - R_S^{\uparrow} + R_L^{\downarrow} - R_L^{\uparrow} \quad (1)$$

and

$$P - Q - G - ET = \Delta S \quad (2)$$

* Corresponding author at: Azadi Avenue, Tehran, PO Box: 11365-11155, Iran.
E-mail address: moghim@sharif.edu.

https://doi.org/10.1016/j.gloplacha.2018.08.013
Received 28 December 2017; Received in revised form 13 August 2018; Accepted 18 August 2018
Available online 24 August 2018
0921-8181/ © 2018 Elsevier B.V. All rights reserved.

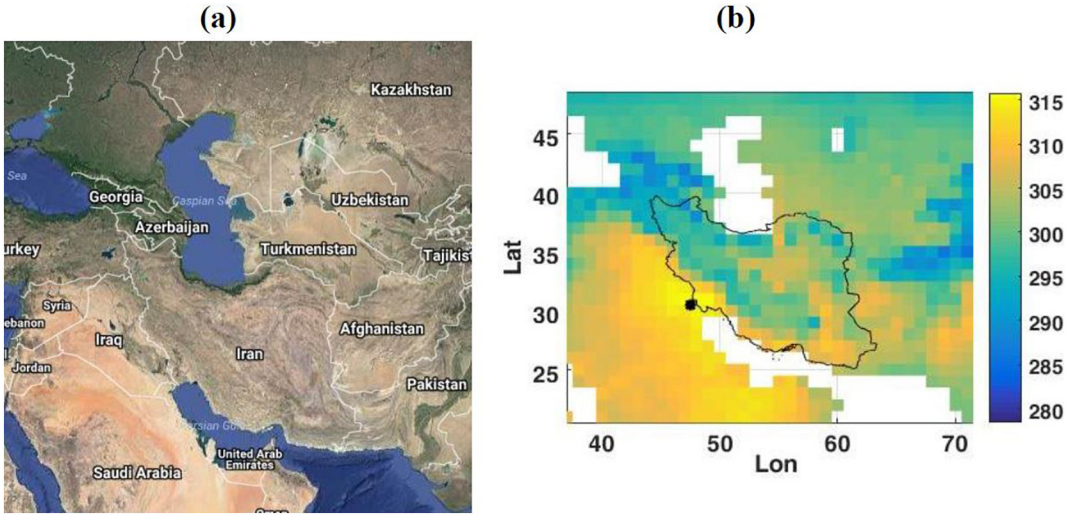

Fig. 1. (a) Map of Iran and Neighbors (obtained from Google Map), (b) Average temperature in August 2015 over Iran and neighboring countries. The black circle shows the place with the maximum temperature.

where R_n is net radiation, $R_S^{\downarrow}$ is downwelling shortwave, $R_S^{\uparrow}$ is upwelling shortwave, $R_L^{\downarrow}$ is downwelling longwave, and $R_L^{\uparrow}$ is upwelling longwave radiation. For further details in Eq. (1), the reader is referred to Moghim et al. (2015). P, Q, G, ET, and ΔS refer to precipitation, runoff, groundwater, evapotranspiration, and storage changes, respectively. Different cloud types with varied features (e.g. albedo, thickness) play a critical role in net radiation changes, which can lead to different precipitation patterns. Increase (decrease) in precipitation can increase (decrease) runoff and soil moisture, which directly influences extreme hydrological events such as flood (drought).

This study focuses on Iran extending from 25°N to 40°N latitude and from 44°E to 64°E longitude (Fig. 1). Iran, the second-largest country in the Middle East, has diverse climate (from arid and semi-arid to humid climate). This country has different land covers such as forest, pasture, agriculture, bare land, desert, and also two main landforms including mountain ranges and seas in north and south. Iran like many other countries in Middle East and North Africa has been experiencing natural and human-induced climate variation, which causes extreme hydrological events such as droughts and floods. While those regions lack climate studies and impact assessments to evaluate current issues and report the results.

Evidence indicates that damages and economic losses from natural disasters are increasing significantly in Iran. For instance, strong storm hit Iran in 2015 that had serious impacts on different provinces. Damages caused by heavy rains in southern Iran costed about 60 million dollars. Floods had severe damages on many houses (at least 900), infrastructure, water and power supply (FloodList, 2008). Iranian Red Crescent reported strong floods and landslides in northwest of Iran that caused loss of life (at least 42) and significant property damages in 2017 (FloodList, 2008). The National Drought Warning and Monitoring Center (NDWMC) reported a 50% decrease in annual precipitation over 40 years in Sistan and Baluchestan Province in southeast of Iran (Financial Tribune, 2015). This reduction leads to severe droughts that influence food quality and quantity, economy, health, and people's livelihood (Provincial Disaster Management Authority, PDMA Balochistan, 2012).

Evidence indicates that Iran is facing more frequent and severe natural disasters and extreme weather events. Communities need to adapt to changes and mitigate damages. This study can provide an integrated assessment of climate variability and its impact on the hydrological cycle in Iran. Section 2 describes methods and data that are used in this work. Changes in the water and energy budget are explained in sections 3 and 4, respectively. Different patterns of hydrometeorological changes are discussed in section 5, followed by their interconnection changes in sections 6. Discussion and concluding remarks are pointed out in Section 7.

2. Methods and data

Climate studies require long-term datasets, which are usually limited in the Middle East. Lack of observed data in Iran affects climate research, impact assessments, and policy-making processes. To reduce the risk of loss and damage from climate change and protect ecosystem and natural resources, we need to use available data and evidence to assess current and projected changes. This study aims to analyze the hydrometeorological variables to clarify connections between climate variations, hydrometeorological changes, and extreme weather events that most regions like Iran have been facing. The analysis of these linkages clarifies how hydrometeorological variables change mutually through the water cycle and energy budget. For the analysis of hydrometeorological variation, reliable climate data are needed. Many studies have used GCMs to analyze climate changes (e.g Trenberth, 2011; Kharin et al., 2007; Liepert and Previdi, 2009, among many others). The large uncertainty associated with the GCMs for climate studies is of great concern (e.g. Deser et al., 2012; Dobler et al., 2012; Solomon et al., 2007, among many others). Thus, this study uses GLDAS product to analyze and assess climate variation over one of the regions in the Middle East (Iran) that has been experiencing many environmental issues due to lack of climate studies. For instance, Lake Urmia in northwest Iran, which was once the second largest saline lake in the world, has been drying fast.

Global Land Data Assimilation System (GLDAS-2.0 and 2.1) product can provide optimal fields of fluxes and water cycle components (Rodell et al., 2004). GLDAS uses data assimilation techniques and integrates satellite data and ground observations into the advanced land surface models (LSMs) including Catchment, Noah, the Community Land Model (CLM), and the Variable Infiltration Capacity (VIC). GLDAS-2.0 is forced by the Princeton meteorological forcing data (Sheffield et al., 2006) and GLDAS-2.1 is forced by the National Oceanic and Atmospheric Administration (NOAA), Global Data Assimilation System (GDAS) atmospheric analysis fields (Derber et al., 1991), the disaggregated Global Precipitation Climatology Project (GPCP) precipitation fields (Adler et al., 2003), and the Air Force Weather Agency's AGRicultural METeorological modeling system (AGRMET) radiation. GLDAS provides a long-term global (excluding Antarctic) dataset extending from 1948 to present at 3-hourly and monthly resolution.

Table 1
Measures (error and correlation ρ) of the GLDAS performance in simulating temperature *T*, precipitation *P*, evaporation *E*, runoff *Q*, and wind over Iran.

	T (K)	P (mm)	E (mm)	Q (mm)	Wind ($m\,s^{-1}$)
Error	1	14	10	0.60	0.70
ρ	0.95	0.67	0.82	0.85	0.88

GLDAS data products are widely used for hydrometeorology and climate studies (Wang et al., 2011; Rodell et al., 2011; Mueller et al., 2011; Rodell and Kato, 2006, among many others). Variables used in this study include temperature, evaporation, precipitation, runoff, wind, downward shortwave and longwave radiation with spatial resolution of about 1°. Using a set of hydrometeorological data from GLDAS can assure us about physical consistency among variables. To verify GLDAS data over the study domain, observations from available local stations are used. Temperature, precipitation, and wind data are obtained from Iran Meteorological Organization (http://irimo.ir). Data for evaporation and runoff are provided by Iran Water Resources Management Company. Since the weather observation stations are generally limited in space and time particularly in Iran, this study uses available observed data to calculate error (difference between model and observation) and correlation of the modeled and observed variables including temperature, precipitation, evaporation, runoff, and wind. Table 1 summarizes measures (error and correlation) of the GLDAS performance over Iran.

Results confirm that GLDAS can work reasonably well and GLDAS outputs are valid over Iran. To better evaluate the gridded GLDAS data, Climate Research Unit dataset (temperature and precipitation) is also used for a comparison. The gridded CRU product is widely used as the observation in many climate studies (Moghim and Bras, 2017; Sheffield et al., 2006; New et al., 2002, among many others). The Climatic Research Unit in the School of Environmental Sciences and the Tyndall Centre at the University of East Anglia, United Kingdom have produced CRU dataset (Harris et al., 2014). The monthly CRU precipitation and temperature (CRU TS 3.24.01, publicly available at http://badc.nerc.ac.uk/data/cru/) for the period of 1948–2016 are regridded to the GLDAS grid to calculate bias and correlation between two products over the study domain. The average biases of temperature and precipitation between two products over all pixels are 0.4 K and 8 mm, respectively. The average correlation of GLDAS and CRU temperature is 0.99 and for the precipitation one is 0.6. The small error and high correlation between GLDAS dataset and local observations (also CRU data) indicate that GLDAS can be properly used for the weather and climate studies over Iran. Thus, this study uses GLDAS product to analyze climate variation in Iran.

To analyze the regional hydrologic cycle, GLDAS data are used to find extremes and trend of hydrometeorological variables including temperature, evaporation, precipitation, runoff, wind, downwelling longwave and shortwave radiation. This data analysis demonstrates how climate variation can lead to environmental hazards.

To examine the rate of hydrometeorological changes, the average changes of variables in the last decade (2010–2017) and monthly anomalies in 2016 relative to the baseline period are computed pixel by pixel over the study domain. The spatial pattern of changes can represent different levels of climate variation over the country. To illustrate the interconnection of these changes, cross correlations of the average changes of the hydrometeorological variables are also calculated. Analysis of these relationships can help to define negative and positive feedbacks in the climate system.

3. Changes in water budget

One of the indicators of climate change is large temperature variations, which has been occurring in past decade. Analysis of GLDAS temperature confirms that Iran has experienced high temperatures. The maximum *T* (315.76 K) in the southwest of Iran (latitude: 30.5°N and longitude: 47.5°E) was the largest value of temperature in 2015 among neighboring countries since 1948 (black circle in Fig. 1b).

The maximum and minimum spatial average of *T* occurs in Aug 2015 and Jan 1964, respectively. The domain average of temperature (*T*) over Iran shows that temperature has upward trend with an increase of 2.7 K per decade (Fig. 2a). Change in temperature affects hydrological cycle and extreme weather events. An increase in temperature causes more evaporation (*E*), which can lead to dryness. This change can increase the risk of heatwaves and droughts.

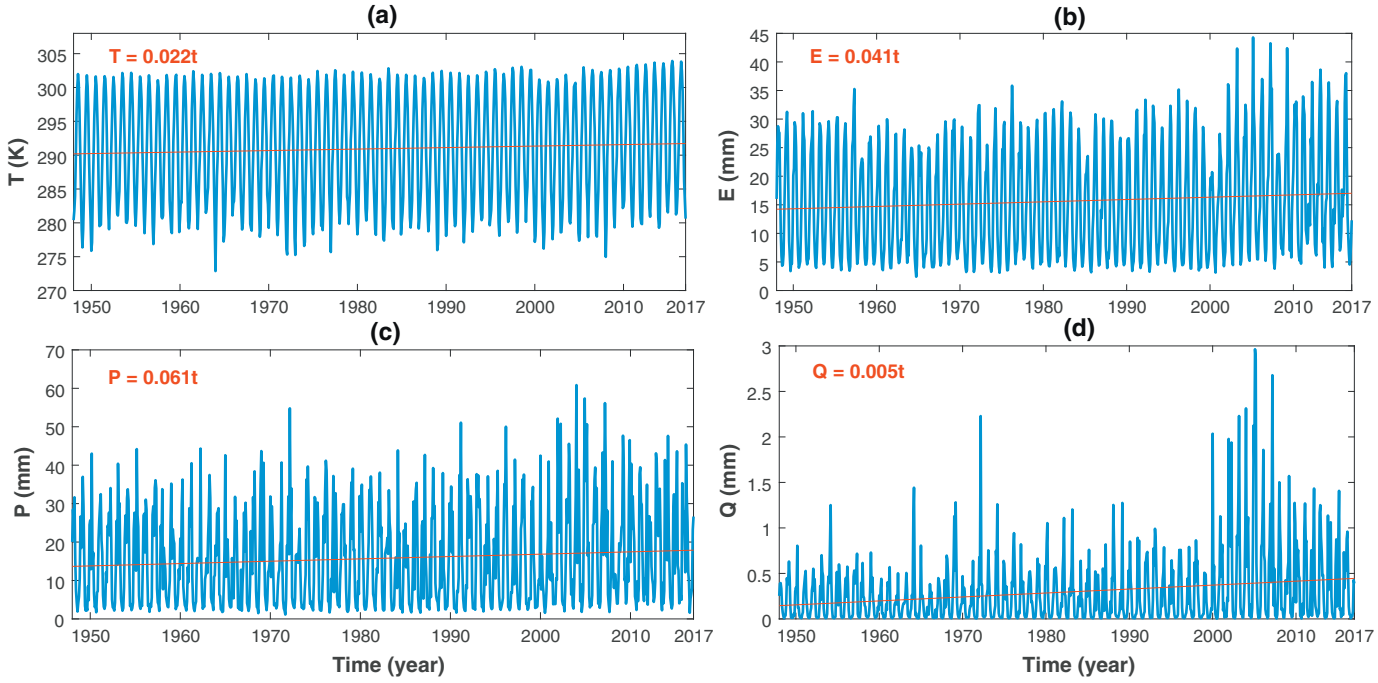

Fig. 2. Time series of domain average of hydrometeorological variables including (a) temperature *T*, (b) evaporation *E*, (c) precipitation *P*, and (d) runoff *Q*.

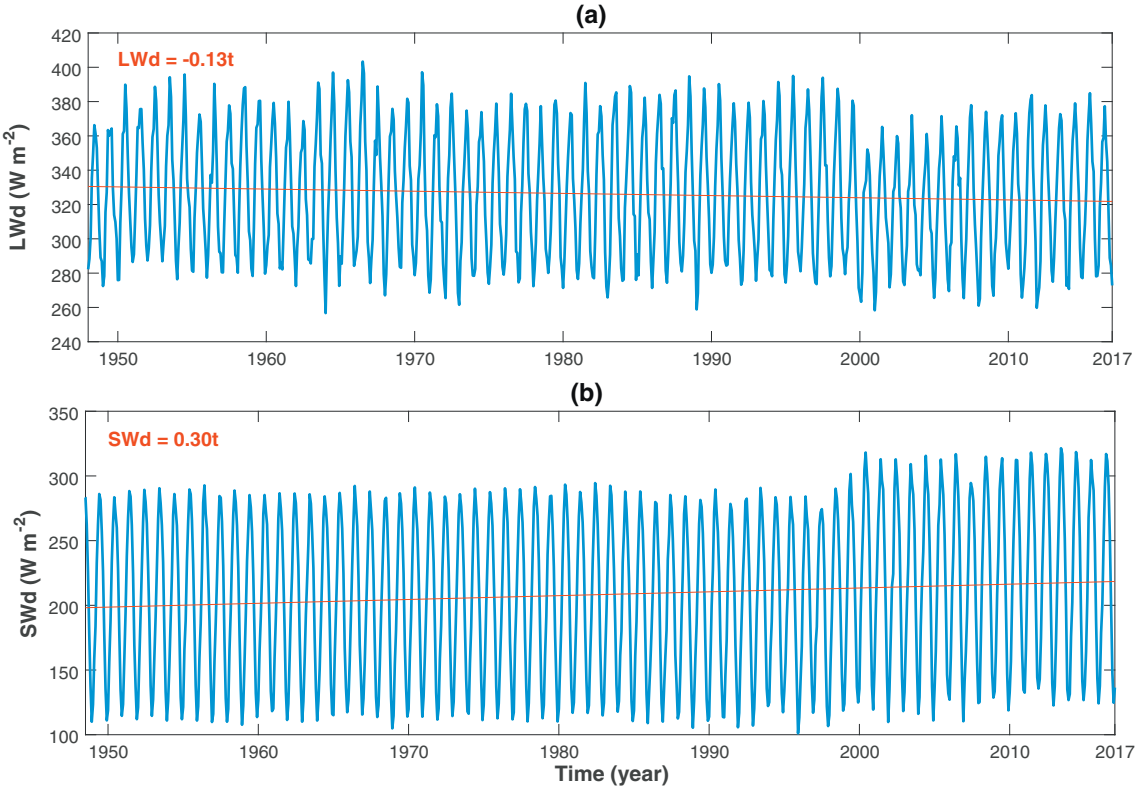

Fig. 3. Time series of domain average of radiation including (a) downward longwave LWd and (b) shortwave SWd radiation.

Fig. 2b shows that the domain average of evaporation has also upward trend with an increase of 4.9 mm per decade. Similar to temperature, maximum evaporation (*E*) occurs in recent years (June 2016) in northwest of Iran. Higher *E* can influence ecosystem functioning. For instance, Lake Urmia in NW of Iran, which was the second saline lake in the world, is drying fast. The size of the lake has been reduced to 10% of its former size during 2000–2014 (Stone, 2015).

Evaporation can provide different feedbacks in the climate system. It increases water vapor as the dominant greenhouse gas (GHG) in the atmosphere. The water vapor can condense into water droplets or ice crystals and produce different types of cloud. Varied clouds can produce different (positive or negative) feedbacks. For instance, high clouds mostly warm the atmosphere and low clouds tend to cool it (Dessler, 2010). Note that the cloud feedbacks are very uncertain (Stephens, 2005) particularly rain clouds. Rain clouds, that are thicker, can reflect more incoming shortwave radiation, thus surface temperature decreases (negative feedback). On the other hand, the thick clouds, that sustain high concentration of water vapor, can trap surface longwave radiation leading to a positive (warming) feedback.

Another indicator of climate change can be high variability of precipitation in different regions. Although Iran has experienced droughts in different years such as severe drought in Isfahan since 2008 (Khodagholi et al., 2014), the domain average of *P* has increased since 1948 (Fig. 2c). This can indicate that different regions have experienced varied hydrological events (heavy rain and drought) in different months. Analysis of the GLDAS precipitation reveals that western Iran is mostly wetter than eastern Iran. On average, northwest (NW) and the Zagros Mountains have experienced larger values of precipitation (and also evaporation). After year 2000, there is an upward and downward trend for spatial average precipitation in fall and winter, respectively. In addition, results show that most precipitation in Iran occurred in month March. The maximum value of precipitation since 1948 was in Dec 2016. Change in precipitation directly influences runoff and water resources (surface and groundwater). Maximum runoff (*Q*) has occurred in month March when maximum precipitation and also snowmelt occur. The maximum *Q* was mostly in northwest and the Zagros Mt. (similar to *P*). Fig. 2d shows an upward trend in spatial average of *Q*, which can indicate an increased threat of flooding. An evidence of this result is the flash floods that occurred in 2017 causing severe damages in terms of loss of lives and properties particularly over northwest (U.S.News, 2017; TEHRANTIMES, 2017).

4. Changes in energy budget

The main driver of the water cycle is energy balance (radiation balance). Climate variation affects radiation including shortwave and longwave radiation. Fig. 3a shows a downward trend in the domain average of downwelling longwave radiation (LWd) over Iran with a decrease of 15.6 $W m^{-2}$ per decade. While, the spatial average of downwelling shortwave radiation (SWd) has an upward trend with an increase of 36 $W m^{-2}$ per decade (Fig. 3b).

Significant changes in radiation can indicate that cloud characteristics (e.g. type and thickness) has been changing, which affects radiation properties including absorptivity, reflectivity, and transmissivity. The analysis of the GLDAS radiation shows that an upward trend of the spatial average of SWd has been increasing. In addition, negative anomalies changed to the positives ones almost in all months after year 2000. Results revealed that the northwest of Iran has experienced both maximum and minimum values of SWd during 1948–2017. On the other hand, the maximum LWd occurred in southern Iran (Persian Gulf coast, Lon: 53.5 N & Lat: 27.5E) in Aug 2011 and minimum of LWd was in northwest in Jan 2017. These recent extremes (max and min) caused by changes in temperature and cloud types are linked to climate variation. Climate variation affects evaporation and humidity through its impact on temperature and water availability, which can lead to produce varied clouds (e.g. different thicknesses) at different levels. Varied clouds have different cloud-radiative forcing (CRF), which drives the hydrologic cycle. Thus, climate variation can impact on cloud types

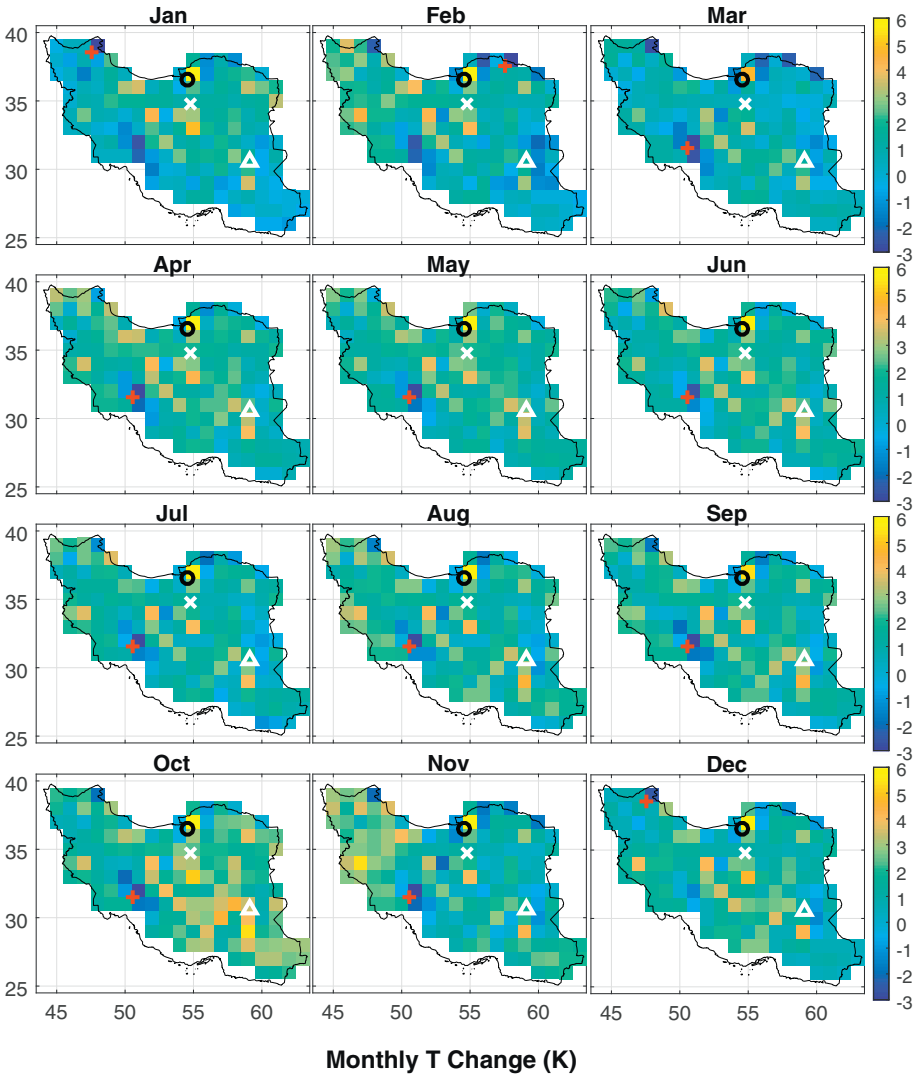

Fig. 4. The differences between monthly averages of temperature *T* in 2010–2017 and the baseline period (2004–2009). The maximum increase and decrease of *T* are illustrated by the black circle and red plus sign, respectively. The white cross and triangle show deserts including Dasht-e Kavir and Dasht-e Lut, respectively. (For interpretation of the references to colour in this figure legend, the reader is referred to the web version of this article.)

(e.g. structure, formation, level, and phase of clouds).

5. Patterns of changes

The analysis of the GLDAS product confirmed that almost all hydrometeorological variables including *T*, *E*, *P*, *Q*, and radiation have changed in Iran. Components of the water cycle are closely tied and any change in one component can directly influence the others. Since the spatial average of extremes (max and min) can balance out, the spatial average of precipitation over different regions with varied precipitation patterns (e.g. heavy rain in one region and no-rain in another region) may not be able to clearly reveal climate variation. In other words, changes can be more noticeable in some months and locations. To better illustrate the spatial changes of hydrometeorological variables, this study uses differences that is defined as the average values in the last decade (2010Jan-2017Jan) minus the average values in the baseline period. Hence, positive and negative values (changes) indicate increases and decreases in the corresponding variables, respectively. To assess climate variability and the rate of hydrometeorological changes, an interval of 2004–2009 is selected as the baseline period. This baseline is also used in other climate studies (e.g. Yang et al., 2018; Ndehedehe et al., 2017; Moiwo et al., 2011; Chandanpurkar et al., 2017, among others). Furthermore, Earth has experienced warmer years since 2010 (NOAA, 2017). Significant changes (warm and cold) are evident in 2010 over many regions in the World (Hansen, 2010; Hausfather, 2011; Giese, 2011). Fig. 4 shows monthly average changes of temperature (2010–2017) relative to the baseline period. In the figure, the circle and plus signs illustrate the locations, where the maximum increase and decrease occur, respectively.

The figure demonstrates that the maximum increase and decrease of temperature for all months occurred in the same locations (Lat: 36.5°E, Lon: 54.5°N for the increase and Lat: 31.5°E, Lon: 50.5°N for the decrease), except for the maximum decrease in winter, which occurred in northwest and northeast. The maximum increase of *T* (6 K) is twice as large as the maximum temperature decrease. The figure verifies that many areas experienced warming in almost all months with stronger signal in some months. For instance, western and eastern regions have experienced more warming than cooling in Nov and Oct, respectively. The deserts including Dasht-e Lut and Kavir (see Fig. 4) have been warming constantly. Warming is more apparent in fall particularly in Oct and Nov. While in month March cooling is more dominant than warming in many regions. Thus, we can conclude that summer started earlier (from spring) and lasted for a longer time (until fall). An increase in duration of hot weather is a key determinant of climate warming.

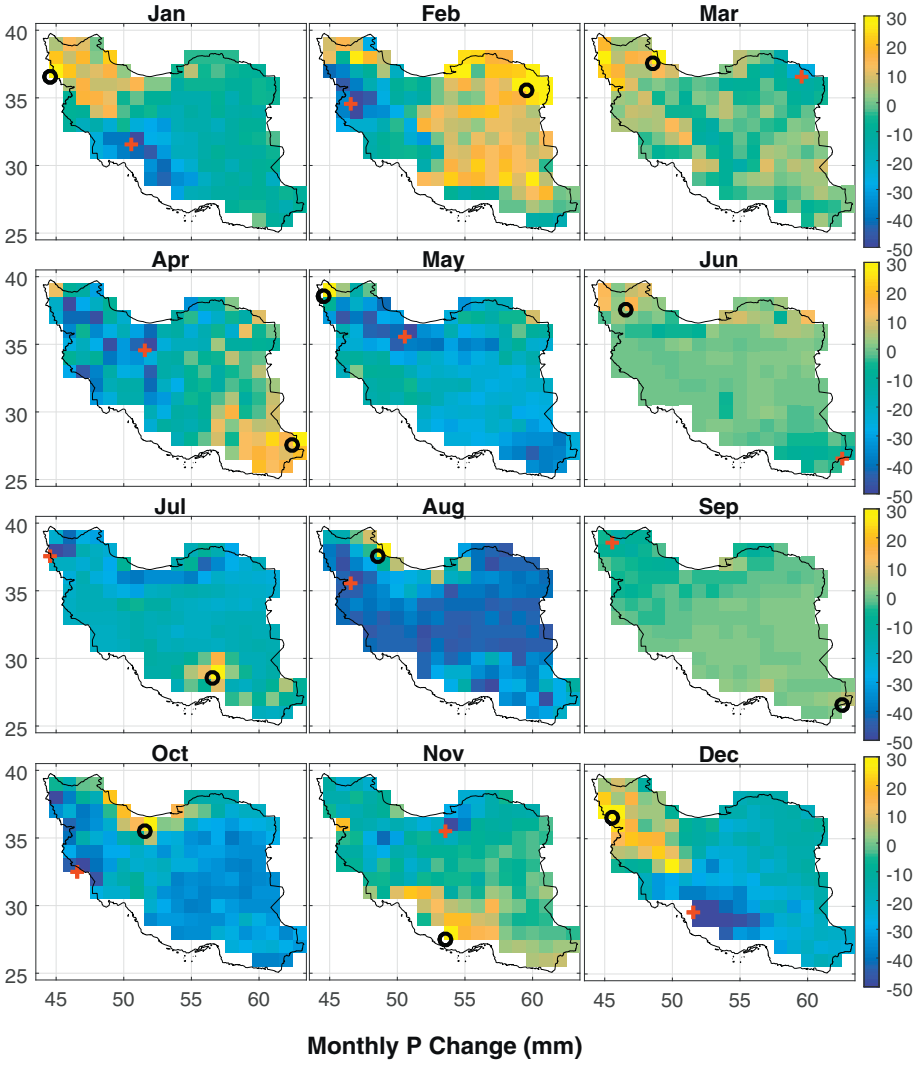

Fig. 5. The differences between monthly averages of precipitation *P* in 2010–2017 and the baseline period (2004–2009). The maximum increase and decrease of *P* are illustrated by the black circle and red plus sign, respectively. (For interpretation of the references to colour in this figure legend, the reader is referred to the web version of this article.)

Prolonged spell of dry and hot weather enhances dryness and drought.

Monthly temperature anomalies of 2016 relative to the baseline period are also estimated. Results revealed that the range of the temperature anomalies in 2016 vary from -5 K to 10 K. This large variability and extreme anomalies in 2016 indicate that we need to expect even more changes in future. The warming anomalies of 2016 were remarkable in fall and winter particularly in Sep, Oct, Dec, and Jan.

The monthly average changes of precipitation are shown in Fig. 5. The maximum monthly increase and decrease of *P* occurred in different locations. This can be due to the fact that different physical features (e.g. topography, land cover, and climatology) of the regions can initiate different mechanisms of precipitation.

The maximum for the average decrease of *P* is almost twice as large as the maximum for the average increase of *P*. A reduction pattern of *P* is dominant in many regions and months particularly in May, Aug, and Oct. An increase in average *P* is more dominant than the decrease of *P* in many regions in March when cooling effect is also dominant (see Fig. 4). World Bank Group also reported that most precipitation occurs in March (World Bank Group, 2017a, 2017b). Fig. 5 illustrates that southern Iran has an increase in average *P* in Nov, while northwest experiences a decrease of average *P* in Nov, which is in contrast to the increase and decrease of average *P* in Dec or Jan over northwest and south, respectively. Note that precipitation has decreased in northwest in most months (Apr, May, Jul, Aug, Sep, Oct, Nov). A clear consequence of precipitation-reduction in northwest is an extreme water level decrease of Lake Urmia. Varied wet or dry anomalies over different regions are evident in different months. For instance, Fig. 5 shows that dry and wet anomalies are distinct mostly in western and eastern regions of Iran in Feb or Apr.

Climate variation, which is linked to the physical features of the regions (e.g., topography, land cover, and dominant weather circulation patterns), varies over the locations from month to month. For instance, results showed that although most regions of the country tend to have a wet-cooling climate in March, many regions have experienced more warming and dry climate in most months (particularly in May, Aug, and Oct). However the spatial average of *P* shows almost an upward trend (Fig. 2c), Fig. 5 illustrates that most regions have experienced dry anomalies. This can indicate that average values of precipitation have decreased but the extremes (e.g. heavy rain and shower) have increased. This is consistent with the results by Trenberth (2011) for global precipitation ("it never rains but it pours!"). Hence, we can conclude that usually there is no certain trend in spatial average of precipitation at the regional and global scale.

The increase and decrease of precipitation in different time can lead to both flood and drought in the same location. In other words, some regions are severely affected by both flood and drought during different

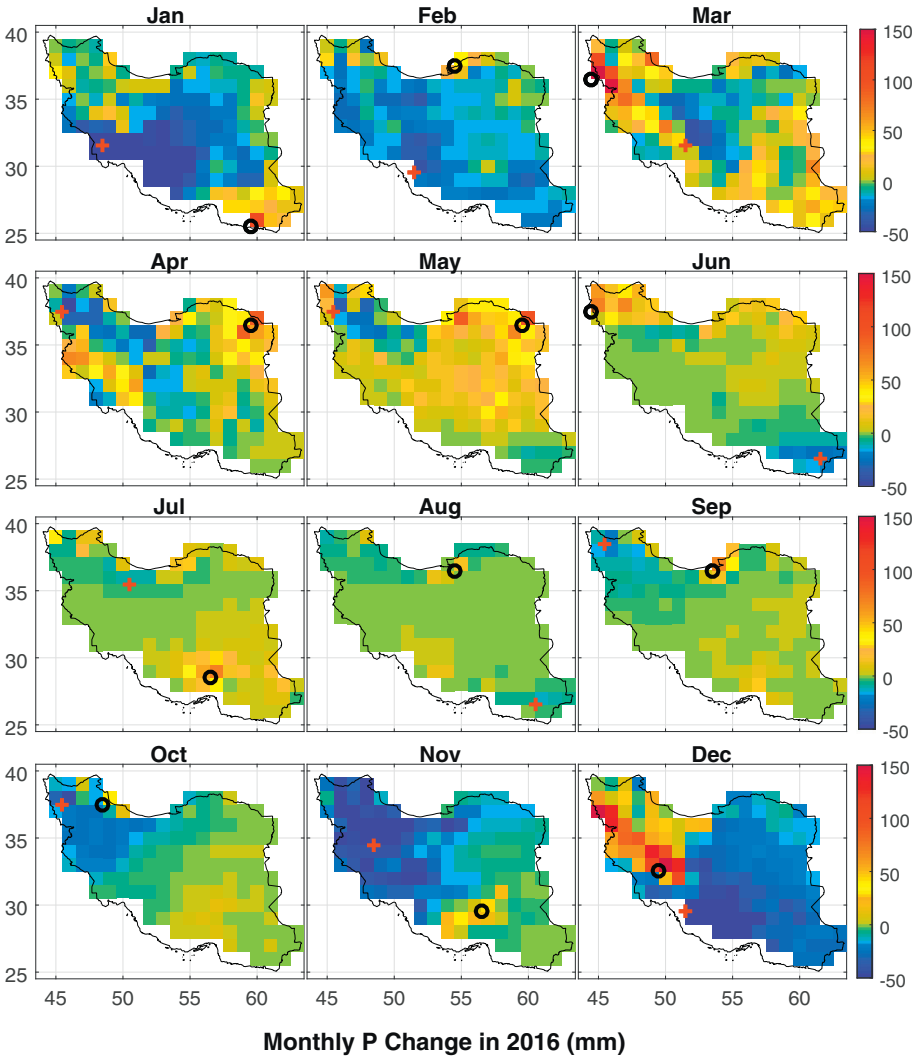

Fig. 6. Monthly anomalies of precipitation *P* in 2016 relative to the baseline period. The maximum increase and decrease of *P* are illustrated by the black circle and red plus sign, respectively. (For interpretation of the references to colour in this figure legend, the reader is referred to the web version of this article.)

seasons. For instance, NDWMC has warned that Sistan and Baluchestan Province faces drought (Financial Tribune, 2015). On the other hand, floods hit this province fairly frequently, which causes severe damages (TEHRANTIMES, 2017; IRNA, n.d.; The Iran Project, n.d.). These dangers can indicate the necessity of having efficient and sustainable plans to control and manage hydrological events including drought and stormwater runoff. Note that the pattern of average changes of runoff closely follows that of precipitation changes. To study the rate of precipitation changes, monthly precipitation anomalies in 2016 are estimated (Fig. 6). However the maximum range of the increase in 2016 precipitation is five times as large as that of the average changes in the period of 2010–2016, only a small part of the country experienced these extreme values of precipitation.

The rate of precipitation changes in 2016 can indicate that we need to expect more extreme precipitation events in future, which is consistent with the results obtained by Fischer and Knutti (2016). In addition, results demonstrate that the pattern of precipitation can change over time. For instance, although many regions experienced average precipitation reduction in May (see Fig. 5), precipitation anomalies in May 2016 increased significantly in many regions (see Fig. 6). In contrast, the positive average anomalies over most regions in Feb (2010–2016) have changed to the negative ones in 2016. This indicates that we need to be prepared for any possible future changes through pre-incident plans. As another water cycle component, the monthly average changes of evaporation are shown in Fig. 7.

The pattern (decrease or increase) of the monthly average changes of evaporation is close to that of precipitation (see Fig. 5) in some months such as Nov, Dec, and Jan (winter). This can indicate that an increase in average precipitation over some regions is followed by higher evaporation. Moreover, some regions experience not only a decrease in average precipitation but also an increase in average evaporation (e.g. northwest and along the Zagros Mountains in Feb). It is evident from Fig. 7 that the average evaporation has increased in mast parts of Iran particularly in northwest and southeast. The pattern of evaporation anomalies in 2016 follows the pattern of average changes of evaporation in the period of 2010–2017 with almost three times larger values. Results confirm that evaporation has a significant upward trend in many regions and months, as a result of increased temperature. Regions that have experienced high evaporation, should expect much higher evaporation in future. High evaporation increases the risk of droughts, heat waves, and wildfires (in particular with precipitation reduction). Positive anomalies and significant upward trend of spatial average evaporation occurred after 2000 in all seasons (excluding winter).

Most extremes (max and min) of hydrometeorological variables occured in northwest. In general, west of Iran (particularly northwest) has experienced more warming anomaly than cooling one in most months (see Fig. 4). On the other hand, precipitation has decreased in

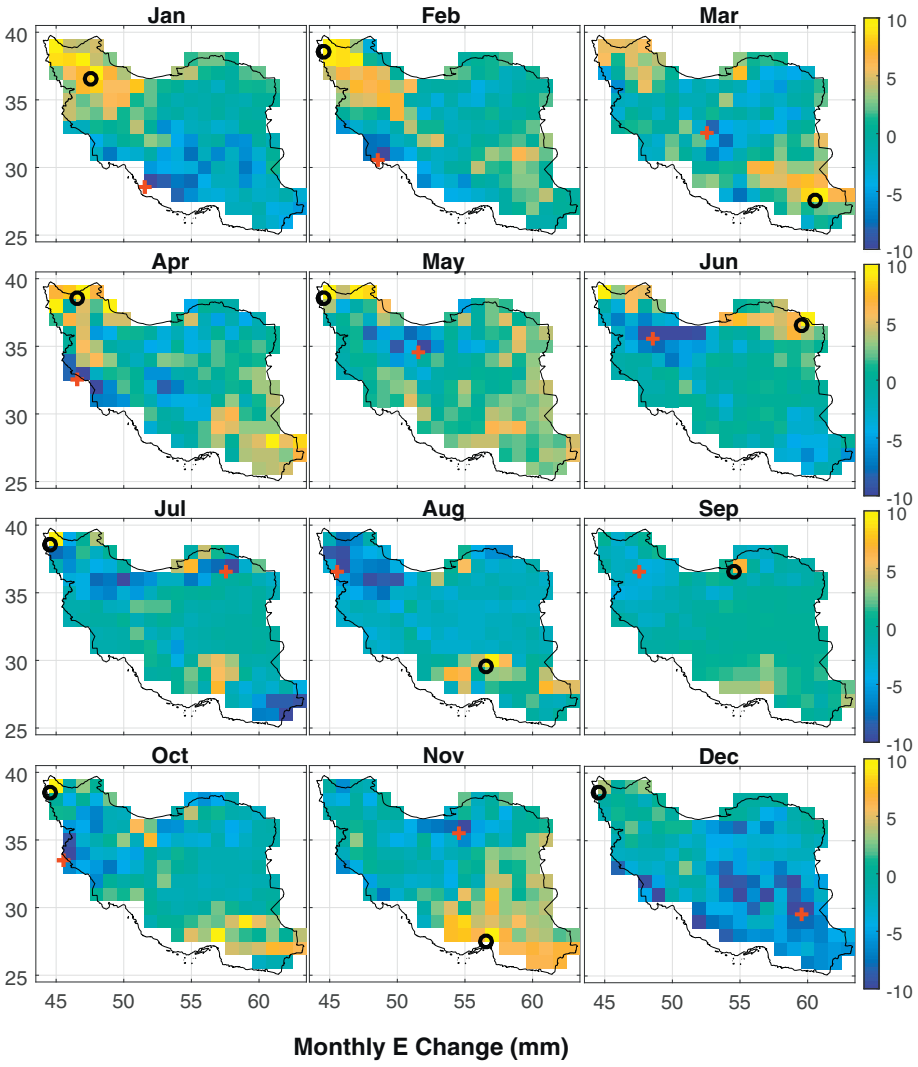

Fig. 7. The differences between monthly averages of evaporation *E* in 2010–2017 and the baseline period (2004–2009). The maximum increase and decrease of *E* are illustrated by the black circle and red plus sign, respectively. (For interpretation of the references to colour in this figure legend, the reader is referred to the web version of this article.)

northwest in most months including Apr, May, Jul, Aug, Sep, Oct, and Nov (see Fig. 5). As a result, climate variation has direct impacts on the water cycle particularly over northwest, where lake Urmia (the second largest saltwater lake in the past) has been considerably shrinking. This highlights the importance of adaptation and mitigation plans to conserve our natural resources.

Monthly average changes of downwelling longwave and shortwave radiation are illustrated in Figs. 8 and 9, respectively.

Results show that all regions have experienced both increases and decreases in average radiation (LWd and SWd) in different months. This can be caused by varied clouds formed at different levels, which provides different albedo and forcing feedbacks. In general, positive differences (increases) in both radiation outweigh negative ones (decreases) in most regions. For instance, an increase in average SWd is dominant in Apr particularly over west and in Dec over east of Iran. To evaluate the rate of changes in downwelling longwave radiation, monthly LWd anomalies in 2016 are estimated (Fig. 10).

Results show that although magnitude of positive anomalies increases relative to the average anomalies during 2010–2016 in most months (see Fig. 8), the pattern of anomalies can completely change. For instance, northwest experienced an increase in average LWd in Nov, Dec, and Jan (see Fig. 8), but these positive anomalies changed to the negative ones in 2016 (see Fig. 10). The change of pattern is also evident in Month Jun. This variation can indicate that we need to consider any possible change of radiation in future, which affects fluxes (sensible, latent, and ground heat flux) and also hydrological cycle.

To better assess spatial climatology in different months, average monthly changes of hydrometeorological variables were also calculated. Analysis of the results revealed that most changes and variability of the variables such as *T*, *E*, *P*, Q, and radiation occurred after year 2000.

6. Interconnection of hydrometeorological changes

Results and evidence revealed widespread variation in hydrometeorological variables such as temperature, precipitation, and radiation over Iran, which can affect weather patterns. Nonlinear interactions between atmosphere and land circulation cause any forcing in the climate system (e.g. change in one variable) directly affects other hydroclimatological variables. In other words, climate system can increase or decrease an initial response to the forcing of the system (positive or negative feedback). These feedbacks affect the rate of hydrometeorological changes. To better evaluate interconnection of the hydrometeorological changes, cross correlation of the average changes of the variables is calculated. Fig. 11a shows the correlation between average changes of temperature and precipitation. The positive values

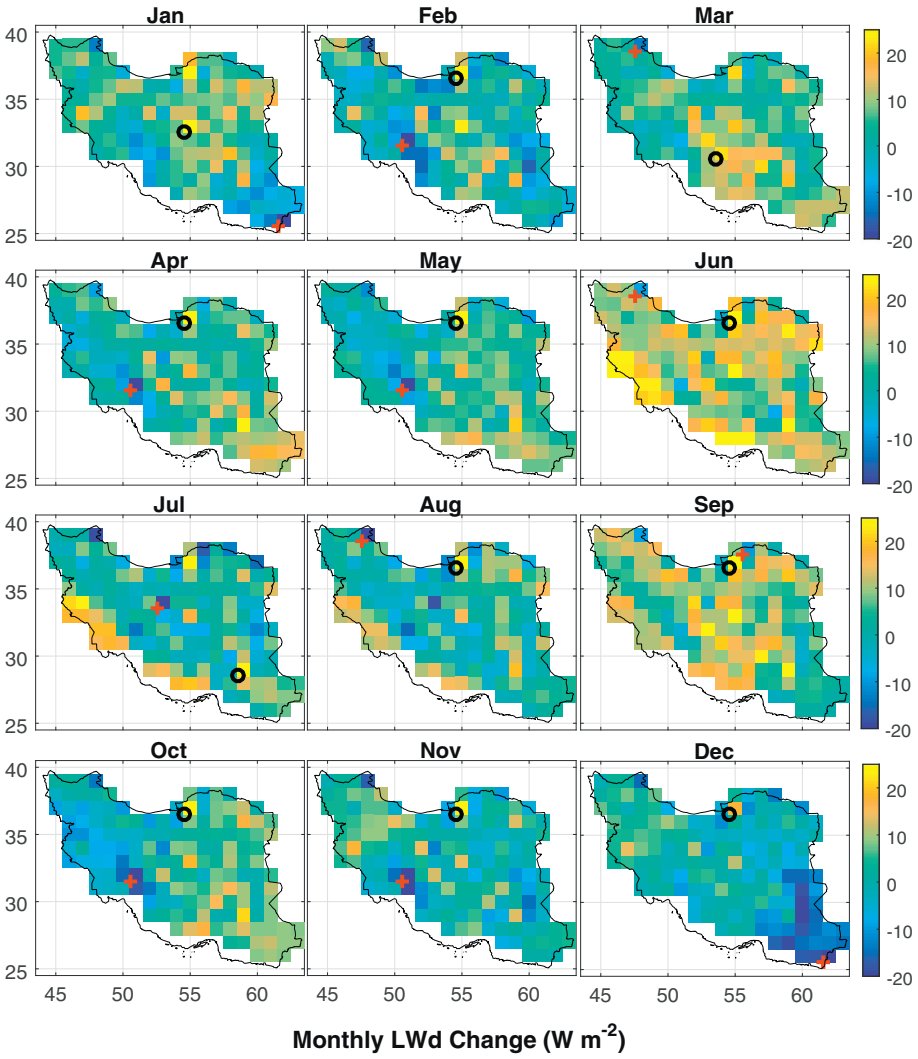

Fig. 8. The differences between monthly averages of downward longwave radiation LWd in 2010–2017 and the baseline period (2004–2009). The maximum increase and decrease of LWd are illustrated by the black circle and red plus sign, respectively. (For interpretation of the references to colour in this figure legend, the reader is referred to the web version of this article.)

(yellowish color) indicate that changes in temperature are positively related to the precipitation changes and negative values (bluish color) show a negative relationship between changes of temperature and precipitation. This figure shows that there is a large negative correlation (-0.4 to -0.8) in most regions except a positive correlation in a small part of northwest Iran. A negative correlation between changes of temperature and precipitation indicates that an increase in T anomaly (with respect to the baseline period) is related to a decrease in P anomaly. In other words, a larger positive deviation of T from the baseline period is linked to a larger negative difference of P from the baseline. Results exhibit a cool-dry anomaly in a small region of southwest, while a hot-dry tendency in most regions is pronounced.

Similarly, the correlation between changes of temperature and surface runoff is negative (mostly -0.3 to -0.6) over all regions. This negative correlation demonstrates that an increase in temperature can be followed by a decrease in runoff.

There are large positive correlations between changes of temperature and radiation particularly LWd in all regions (Fig. 11b and c). While some regions such as northwest and along the Zagros Mountains have a relatively smaller positive correlation (see Fig. 11c). This pattern can refer to different physical features of the domains (e.g., topography, land cover, and climatology). A strong positive correlation between changes of temperature and radiation (downward longwave and shortwave radiation) can be due to the reason that warming influences cloud types and thus cloud forcing and this can amplify initial responses to increased temperature. Changes in temperature and radiation can also affect precipitation types and distribution. Difficulties in cloud analysis remain an area of concern in assessing impacts of climate variation on the precipitation pattern. Although results reveal positive temperature-radiation feedback, climate feedback loops are so complex and still it is not well determined and understood. Most initial responses to the forcing of the system lead to both positive and negative feedbacks; while the final pure and net feedback is difficult and sometimes impossible to be deduced. For instance, climate warming (higher temperature) increases evaporation and atmospheric water vapor (as one of the main GHGs), which can trap longwave radiation (heat), and thus increases warming (positive feedback). On the other hand, atmospheric water vapor can produce clouds with high albedo, which are able to reflect more incoming solar radiation, and thus reduces warming (negative feedback).

The energy budget (incoming and outgoing radiation) is closely tied to the hydrologic cycle. Uneven distribution of energy in particular solar radiation over different regions causes atmospheric circulation and winds, which transfer heat and moisture. To evaluate the impact of warming on the wind as the main driver of atmospheric circulation, the cross correlation between changes of temperature and wind is

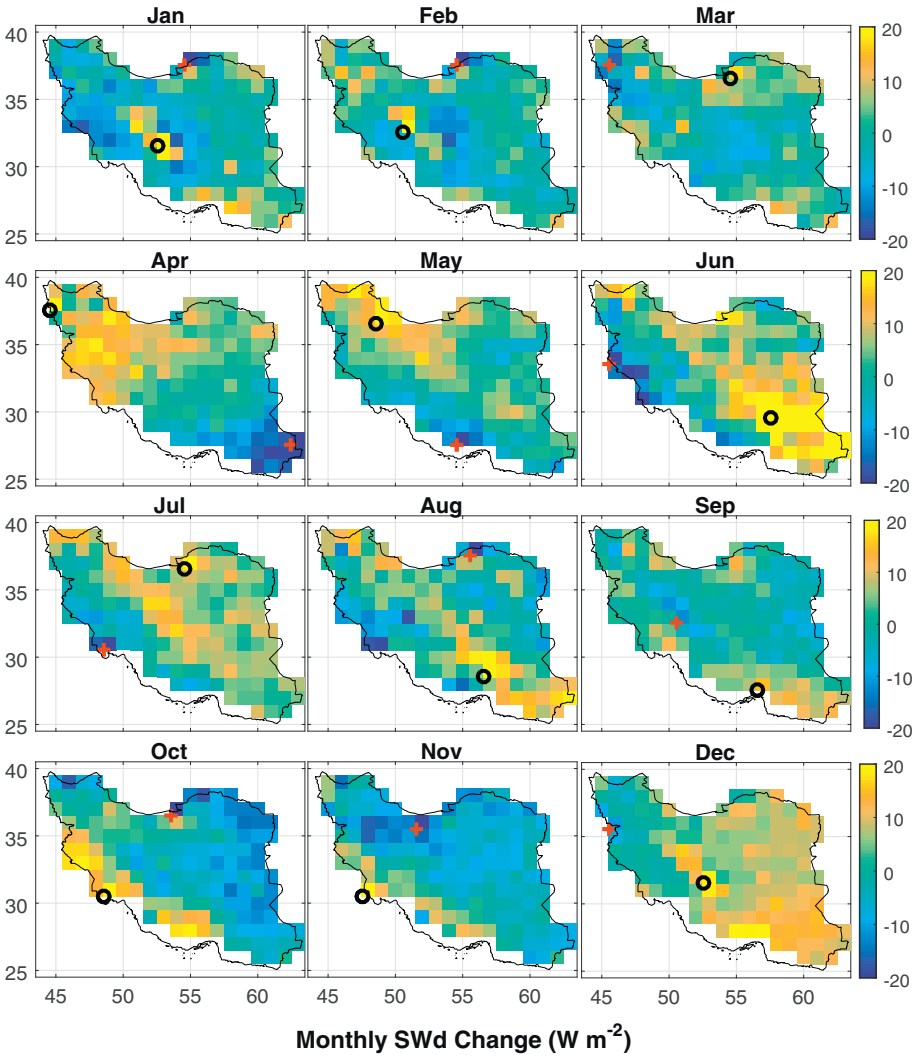

Fig. 9. The differences between monthly averages of downward shortwave radiation SWd in 2010–2017 and the baseline period (2004–2009). The maximum increase and decrease of SWd are illustrated by the black circle and red plus sign, respectively. (For interpretation of the references to colour in this figure legend, the reader is referred to the web version of this article.)

calculated (Fig. 11d). Fig. 11d shows that most regions have positive correlations. In other words, higher temperatures agitate and amplify the wind speed mostly over northeast and southwest. An increase in wind can cause extreme hydrological events (e.g. storm). In addition, high-speed winds can transport dust and aerosol. Most regions in Iran have been experiencing more intense and frequent dust storm. For instance, Ahwaz Monitor Information Center stated emergency condition of sandstorm that covered Ahwaz in southwest in Jan 2017 (Ahwaz Monitor, n.d.). This severe dust storm, which reduced vision to less than five meters, caused power and water cut off, flight cancellations, and breathing problems (Financial Tribune, 2015; The New York Times, 2017).

Changes in temperature and evaporation have direct impacts on atmospheric instability characterized by sensible and latent heat flux, which affect the turbulence formation and severe storm. Trenberth et al. (2003) also pointed out that an additional latent heat energizes storms and increases moisture flux convergence, which is consistent with the phenomenon explained by Liu et al. (2009). Strong positive correlation between temperature and wind changes and also large negative correlation between temperature and precipitation changes over southwest of Iran indicates that warming can strengthen dry winds. These warm and dry winds can characterize strong sand and dust storms. Evidence also confirms more frequent intense dust storm on west of Iran (Naimabadi et al., 2016; Najafi et al., 2014). Indeed, besides energy balance (radiation), atmospheric circulation (wind) is also interconnected with the hydrologic cycle and hydrometeorological variables are closely interlinked. Analysis of these linkages is essential for the sustainable management to regulate and sustain natural resources.

7. Discussion and concluding remarks

This work used GLDAS product to investigate hydrometeorological variation during Jan1948-Jan2017 in Iran. Analysis of the results provided evidence of high climate variation over Iran. Although this study assessed climate variability during 1948–2017, hydrometeorological changes in this long period can indicate the possible climate change in future. Results demonstrated that the average temperature (the main indicator of climate change) over Iran has increased about 2.7 K per decade. The average precipitation and evaporation have also increased about 7.3 mm and 4.9 mm per decade, respectively. Results showed that although a strong increase in heavy precipitation occurred in a small portion of the country, many regions experienced a decrease of precipitation in 2016. Indeed, climate variation alters the intensity and frequency of precipitation (extremes), which can increase the risk of floods and droughts.

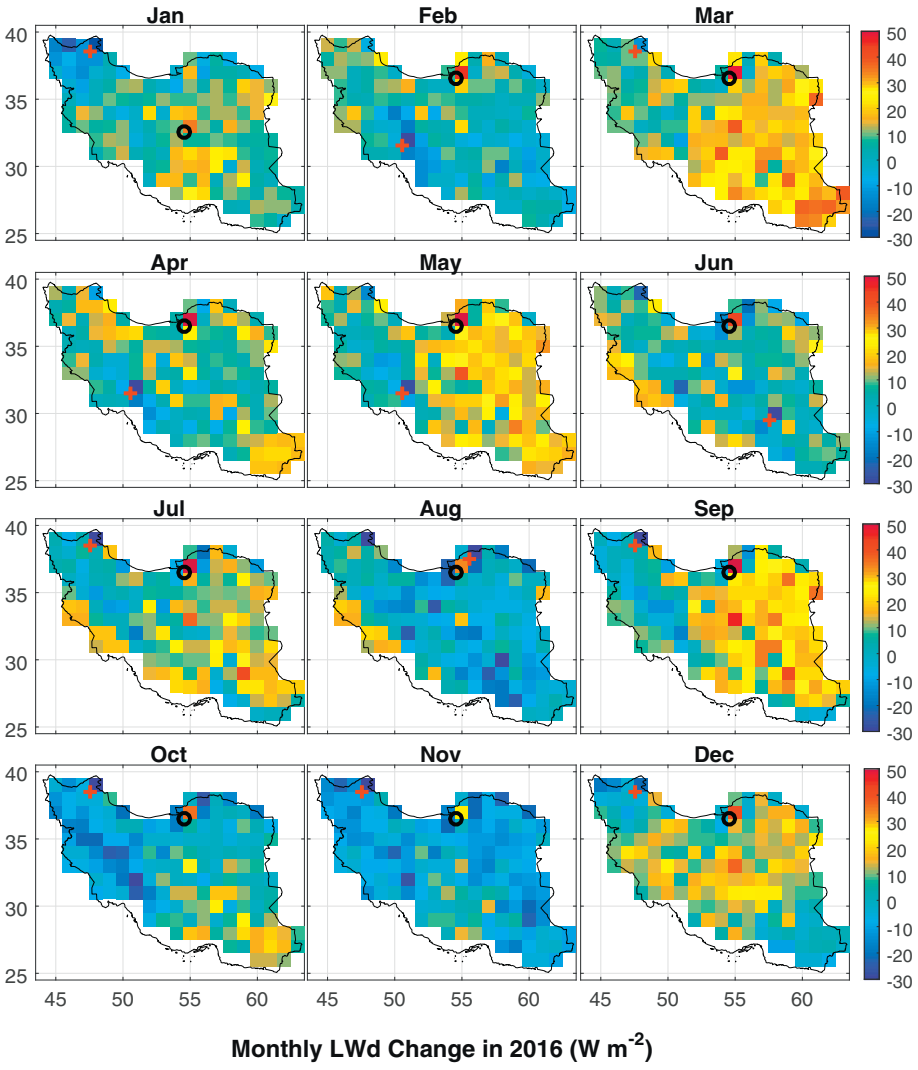

Fig. 10. Monthly anomalies of downward longwave radiation LWd in 2016 relative to the baseline period. The maximum increase and decrease of LWd are illustrated by the black circle and red plus sign, respectively. (For interpretation of the references to colour in this figure legend, the reader is referred to the web version of this article.)

In addition, results showed that an increase in average temperature is associated with a decrease in average precipitation. This negative correlation between temperature and precipitation changes can be a warning sign indicating that more warming can be accompanied by the precipitation-reduction almost all over the country. Furthermore, evaporation values had the most changes. Thus, evaporation can be defined as the key indicator of the water cycle for assessing climate-induced hydrological variation.

A clear evidence of high climate variation in Iran is environmental crisis in Lake Urmia located in northwestern Iran, where most extremes (max and min) of hydrometeorological variables have occurred. This lake that was once the second largest saline lake in the world, has been drying fast.

The range of changes (increase or decrease) in the hydrometeorological variables varies in different regions and months. Indeed, different physical features of the regions that affect climate variation, are reflected in the results. A very robust finding is that although different regions in Iran have experienced varied climate patterns, most parts of Iran tend to have a warming-dry anomaly in most months, which is even more evident in 2016. These tendencies arise from the increase in temperature, evaporation, and intensity of extreme precipitation and the decrease in average values of precipitation.

A significant increase of hydroclimatological anomalies (the 2016 anomalies relative to the average anomalies) can reveal that we need to expect a higher rate of hydrometeorological changes in future. In other words, climate variation will cause more extreme events and thus more severe damages. Communities should be prepared for anticipated hazards and improve their resiliency through adaptation and mitigation plans.

This work provides an integrated view of interlinkages of water cycle components and its drivers (e.g. radiation). Analysis of these linkages is essential for climate variation assessment. Results of this study that are expected to continue in future can be a valuable source to evaluate climate change projections and hydrological hazards.

Acknowledgment

The data used in this study were acquired as part of the mission of NASA's Earth Science Division and archived and distributed by the Goddard Earth Sciences (GES) Data and Information Services Center (DISC). I am thankful to Ms. Hualan Rui for her help and suggestions in this work. I also recognize the UNESCO Chair in Water and Environment Management for Sustainable Cities in Sharif University of Technology for the support during this study.

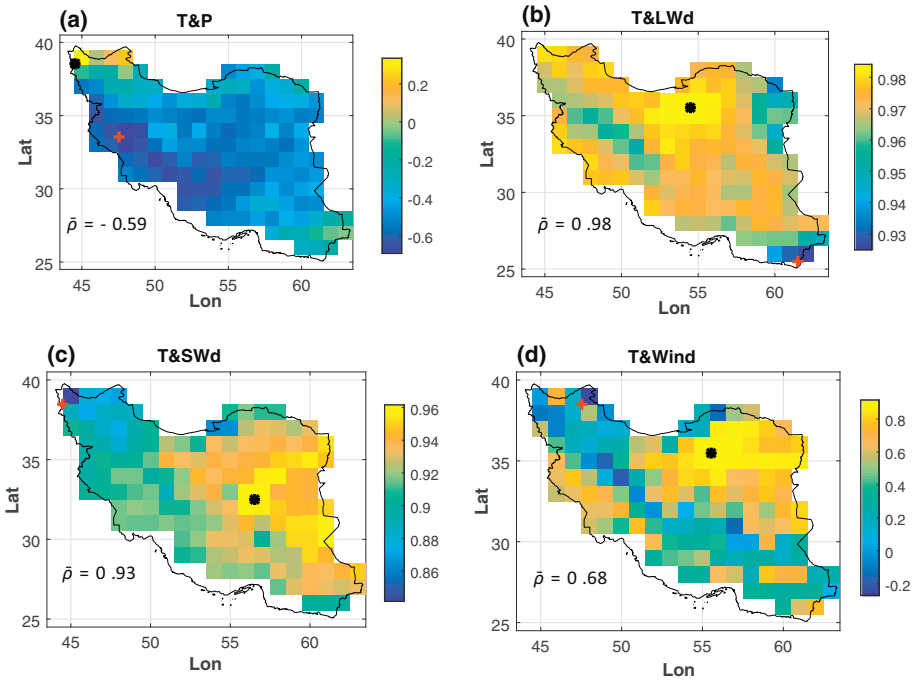

Fig. 11. Correlation between average anomalies of temperature and (a) precipitation T&P, (b) downward longwave radiation T&LWd, (c) shortwave radiation T&SWd, and (d) wind T&Wind. The maximum positive and negative correlations are illustrated by the black circle and red plus sign, respectively. (For interpretation of the references to colour in this figure legend, the reader is referred to the web version of this article.)

References

Abbaspour, K.C., Faramarzi, M., Ghasemi, S.S., Yang, H., 2009. Assessing the impact of climate change on water resources in Iran. Water Resour. Res. 45, W10434.

Adler, R.F., Huffman, G.J., Chang, A., Ferraro, R., Xie, P., Janowiak, J., Rudolf, B., Schneider, U., Curtis, S., Bolvin, D., Gruber, A., Susskind, J., Arkin, P., Nelkin, E., 2003. The Version 2 Global Precipitation Climatology Project (GPCP) Monthly Precipitation Analysis (1979-Present). J. Hydrometeorol. 4, 1147–1167.

Ahwaz Monitor Retrieved from. http://www.ahwazmonitor.info/new/severe-sandstorms-blanket-ahwaz-for-a-week-causing-deaths-illness/.

Bathiany, S., Dakos, V., Scheffer, M., Lenton, T.M., 2018. Climate models predict increasing temperature variability in poor countries. Sci. Adv. 4, eaar5809.

Chandanpurkar, H.A., Reager, J.T., Famiglietti, J.S., Syed, T.H., 2017. Satellite- and Reanalysis-Based Mass Balance Estimates of Global Continental Discharge (1993–2015). J. Clim. 30, 8481–8495.

Delju, A.H., Ceylan, A., Piguet, E., Rebetez, M., 2013. Observed climate variability and change in Urmia Lake Basin, Iran. Theor. Appl. Climatol. 111, 285–296.

Derber, J.C., Parrish, D.F., Lord, S.J., 1991. The new global operational analysis system at the National Meteorological Center. Weather Forecast. 6, 538–547.

Deser, C., Phillips, A., Bourdette, V., Teng, H., 2012. Uncertainty in climate change projections: The role of internal variability. Clim. Dyn. 38, 527–546.

Dessler, A.E., 2010. A determination of the cloud feedback from climate variations over the past decade. Science 330, 1523–1527.

Dobler, C., Hagemann, S., Wilby, R.L., Stötter, J., 2012. Quantifying different sources of uncertainty in hydrological projections in an Alpine watershed. Hydrol. Earth Syst. Sci. 16, 4343–4360.

Financial Tribune, 2015. First Iranian English Economic Daily. Retrieved from. https://financialtribune.com/articles/people/10353/sistan-baluchestan-facesdrought.

Fischer, E.M., Knutti, R., 2016. Observed heavy precipitation increase confirms theory and early models. Nat. Clim. Chang. 6, 986–991.

FloodList, 2008. Reporting floods and flooding news since 2008. Retrieved from. http://floodlist.com/.

Giese, A., 2011. Global Temperature, Eco-Economy Indicator. Earth Policy Institute Retrieved from. http://www.earth-policy.org.

Harris, I., Jones, P.D., Osborn, T.J., Lister, D.H., 2014. Updated high-resolution grids of monthly climatic observations the CRU TS3.10 dataset. Int. J. Climatol. 34, 623–642.

Hausfather, Z., 2011. Global Temperature in 2010: Is it the Hottest Year on Record, and Does it Matter? YALE Climate Connections. Retrieved from. https://www. https://www.yaleclimateconnections.org/2011/02/global-temperature-in-2010-hottest-year/.

IRNA Islamic Republic News Agency. Retrieved from. http://www.irna.ir/en/.

Jamali, S., Abrishamchi, A., Madani, K., 2013. Climate Change and Hydropower Planning in the Middle East: Implications for Iran's Karkheh Hydropower Systems. J. Energy Eng. 139.

Kharin, V.V., Zwiers, F.W., Zhang, X., Hegerl, G.C., 2007. Changes in temperature and precipitation extremes in the IPCC ensemble of global coupled model simulations. J. Clim. 20, 1419–1444.

Khodagholi, M., Saboohi, R., Eskandari, Z., 2014. Analysing Drought Past Trend and Forecasting its Future in Isfahan Province. JWSS 18, 367–379.

Liepert, B.G., Previdi, M., 2009. Do models and observations disagree on the rainfall response to global warming? J. Clim. 22, 3156–3166.

Liu, S.C., Fu, C., Shiu, C.J., Chen, J.P., Wu, F., 2009. Temperature dependence of global precipitation extremes. Geophys. Res. Lett. 36, L17702.

Moghim, S., Bras, R.L., 2017. Bias correction of climate modeled temperature and precipitation using Artificial Neural Networks. J. Hydrometeorol. 18, 1867–1884.

Moghim, S., Bowen, A.J., Sarachi, S., Wang, J., 2015. Retrieval of Hourly Records of Surface Hydrometeorological Variables Using Satellite Remote Sensing Data. J. Hydrometeorol. 16, 147–157.

Moiwo, J.P., Yang, Y., Tao, F., Lu, W., Han, S., 2011. Water storage change in the Himalayas from the Gravity Recovery and Climate Experiment (GRACE) and an empirical climate model. Water Resour. Res. 47, W07521.

Mostafavi, P.G., Fatemi, S.M.R., Shahhosseiny, M.H., Hoegh-Guldberg, O., Loh, W.K.W., 2007. Predominance of clade D Symbiodinium in shallow-water reef-building corals off Kish and Larak Islands (Persian Gulf, Iran). Mar. Biol. 153, 25–34.

Motagh, M., Djamour, Y., Walter, T.R., Wetzel, H.U., Zschau, J., Arabi, S., 2007. Land subsidence in Mashhad Valley, northeast Iran: results from InSAR, levelling and GPS. Geophys. J. Int. 168, 518–526.

Mueller, B., Seneviratne, S.I., Jimenez, C., Corti, T., Hirschi, M., Balsamo, G., Beljaars, A., Betts, A.K., Ciais, P., Dirmeyer, P., Fisher, J.B., Guo, Z., Jung, M., Kummerow, C.D., Maignan, F., McCabe, M.F., Reichle, R., Reichstein, M., Rodell, M., Rossow, W.B., Sheffield, J., Teuling, A.J., Wang, K., Wood, E.F., 2011. Evaluation of global observations-based evapotranspiration datasets and IPCC AR4 simulations. Geophys. Res. Lett. 38, L06402.

Naimabadi, A., Ghadiri, A., Idanie, E., Babaei, A.A., Alavi, N., Shirmardi, M., Khodadadi, A., Marzouni, M.B., Ankali, K.A., Rouhizadeh, A., Goudarzi, G., 2016. Chemical composition of PM10 and its in vitro toxicological impacts on lung cells during the Middle Eastern Dust (MED) storms in Ahvaz, Iran. Environ. Pollut. 211, 316–324.

Najafi, M.S., Khoshakhllagh, F., Zamanzadeh, S.M., Shirazi, M.H., Samadi, M., Hajikhani, S., 2014. Characteristics of TSP Loads during the Middle East Springtime Dust Storm (MESDS) in Western Iran. Arab. J. Geosci. 7, 5367–5381.

Ndehedehe, C.E., Awange, J.L., Kuhn, M., Agutu, N.O., Fukuda, Y., 2017. Analysis of hydrological variability over the Volta river basin using in-situ data and satellite observations. J. Hydrol.: Regional Studies 12, 88–110.

New, M., Lister, D., Hulme, M., Makin, I., 2002. A high-resolution data set of surface climate over global land areas. Clim. Res. 21.

NOAA, 2017. In: National Centers for Environmental Information (Ed.), State of the Climate: Global Climate Report for Annual 2016, published online January 2017, retrieved on April 29, 2018 from. https://www.ncdc.noaa.gov/sotc/global/201613.

PDMA Balochistan, 2012. Provincial Disaster Management Authority. Retrieved from. http://pdma.gob.pk/?p=54.

Rodell, M., Kato, H., 2006. GLDAS output supports CEOP studies, CEOP Newsletter. pp. 10.

Rodell, M., Houser, P.R., Jambor, U., Gottschalck, J., Mitchell, K., Meng, C.-J., Arsenault, K., Cosgrove, A., Radakovich, J., Bosilovich, M., Entin, J.K., Walker, J.P., Lohmann, D., Toll, D., 2004. The Global Land Data Assimilation System. Bull. Amer. Meteor. Soc. 85, 381–394.

Rodell, M., McWilliams, E.B., Famiglietti, J.S., Beaudoing, H.K., Nigro, J., 2011. Estimating evapotranspiration using an observation based terrestrial water budget. Hydrol. Proc. 25, 4082–4092.

Sheffield, J., Goteti, G., Wood, E.F., 2006. Development of a 50-yr high-resolution global dataset of meteorological forcings for land surface modeling. J. Clim. 19, 3088–3111.

Shinn, E.A., 1976. Coral reef recovery in Florida and the Persian Gulf. Environ. Geol. 1,

241–254.
Solomon, S., Qin, D., Manning, M., Chen, Z., Marquis, M., Averyt, K., Tignor, M.M.B., Miller Jr., H.L., 2007. Climate Change 2007: The Physical Science Basis. Cambridge University Press (996 pp).
Stephens, G.L., 2005. Cloud Feedbacks in the Climate System: A Critical Review. J. Clim. 18, 237–273.
Stone, R., 2015. Saving Iran's great salt lake. Science 349, 1044–1047.
Tabari, H., Aghakouchak, A., Willems, P., 2014. A perturbation approach for assessing trends in precipitation extremes across Iran. J. Hydrol. 519, 1420–1427.
TEHRANTIMES, 2017. Iran's Leading International Daily. Retrieved from. http://www.tehrantimes.com/news/416617/Flash-flood-hits-northern-Iran.
The Iran Project Retrieved from. http://theiranproject.com/blog/2017/01/28/six-die-sistan-baluchestan-floods/.
The New York Times, 2017. Protests in Iranian City Where 'Everything Is Covered in Brown Dust. Retrieved from. https://www.nytimes.com/2017/02/19/world/middleeast/iran-ahvaz-pollution-protests.html.
Tourian, M.J., Elmi, O., Chen, Q., Devaraju, B., Roohi, Sh., Sneeuw, N., 2015. A space-borne multisensor approach to monitor the desiccation of Lake Urmia in Iran. Remote Sens. Environ. 156, 349–360.
Trenberth, K.E., 2011. Changes in precipitation with climate change. Clim. Res. 47, 123–138.
Trenberth, K.E., Dai, A., Rasmussen, R.M., Parsons, D.B., 2003. The changing character of precipitation. Bull. Am. Meteorol. Soc. 84, 1205–1217.
U.S.News, 2017. Retrieved from. https://www.usnews.com/news/world/articles/2017-08-12/state-tv-flash-floods-kill-12-in-northwest-iran.
Wang, F., Wang, L., Koike, T., Zhou, H., Yang, K., Wang, A., Li, W., 2011. Evaluation and application of a fine-resolution global data set in a semiarid mesoscale river basin with a distributed biosphere hydrological model. J. Geophys. Res. 116, D21108.
World Bank Group, 2017a. Beyond Scarcity: Water Security in the Middle East and North Africa. In: MENA Development Series. World Bank, Washington, DC. License: Creative Commons Attribution CC BY 3.0 IGO.
World Bank Group, 2017b. Climate Change Knowledge Portal. Retrieved from. http://sdwebx.worldbank.org/climateportal/index.cfm?page=country_historical_climate&ThisCCode=IRN.
Yang, P., Zhan, C., Xia, J., Han, J., Hu, S., 2018. Analysis of the spatiotemporal changes in terrestrial water storage anomaly and impacting factors over the typical mountains in China. Int. J. Remote Sens. 39, 505–524.
Zarghami, M., 2011. Effective watershed management; Case study of Urmia Lake, Iran. Lake and Reservoir Management 27, 87–94.